

# Detailed Structure of a CDW in a Quenched Random Field

J.D. Brock, A.C. Finnefrock, K.L. Ringland, and E. Sweetland

*School of Applied and Engineering Physics*

*Cornell University, Ithaca, New York 14853*

(June 21, 2021)

## Abstract

Using high resolution x-ray scattering, we have measured the structure of the  $\mathbf{Q}_1$  CDW in Ta-doped NbSe<sub>3</sub>. Detailed line shape analysis of the data demonstrates that two length scales are required to describe the phase-phase correlation function. Phase fluctuations with wavelengths less than a new length scale  $a$  are suppressed and this  $a$  is identified with the amplitude coherence length. We find that  $\xi_{\mathbf{a}^*} = 34.4 \pm 10.3\text{\AA}$ . Implications for the physical mechanisms responsible for pinning are discussed.

PACS numbers: 78.70.Ck, 71.45.Lr, 64.60.Cn

During the past twenty years, the influence of random disorder on phase transitions has been studied extensively. Disorder can be formally described as randomness in either the interaction strength [1] or the field conjugate to the order parameter [2]. It is widely believed that a small amount of randomness in the interactions is irrelevant. Random fields, on the other hand, have dramatic consequences. In their seminal paper, Imry and Ma [2] suggested that a random field should cause the lower marginal dimensionality  $d_\ell$  to rise from 2 to 4 for systems with continuous symmetry. Here,  $d_\ell$  is the dimensionality below which the system cannot sustain long-range order (LRO) at finite temperatures [3]. This loss of LRO has been observed in a wide variety of systems. In particular, the structures of the charge-density waves (CDW's) found in the quasi-one-dimensional metal NbSe<sub>3</sub> do not exhibit LRO [4,5].

For mathematical simplicity, the quenched random field is frequently assumed to be a time-independent random Gaussian variable satisfying  $\langle h(\mathbf{r}) \rangle = 0$  and  $\langle h(\mathbf{r})h(\mathbf{r}') \rangle = n_i h_0^2 \delta^d(\mathbf{r} - \mathbf{r}')$  where  $n_i$  is the number density of impurity atoms and  $h_0$  gives the strength of the pinning interaction. In the general case, scattering from a random structure is characterized by an exponentially decaying correlation function [6]. For the specific case of CDW systems, one expects an exponential decay of the correlations between static fluctuations in the phase of the CDW order parameter [7,8].

In this paper, we report the results of a detailed high resolution x-ray scattering study of the static phase correlations of the  $\mathbf{Q}_1$  CDW in Ta-doped NbSe<sub>3</sub>. The experiments clearly show that phase fluctuations with high spatial frequency components are suppressed; therefore, the destruction of LRO by the random field is suppressed on length scales less than  $\approx 75$  Å. These results are explained using the standard Ginzburg-Landau phase Hamiltonian with a Gaussian random pinning field [7,8]. This new length scale is then related directly to the amplitude coherence length. We conclude with a brief discussion of the implications for physical models of the pinning mechanism.

The obvious way to study the interaction between a CDW and a quenched random distribution of impurity atoms is to dope crystals with impurities and study how the ordering varies with impurity concentration and type. Over the last decade a large number of such

studies have been reported [9,10]. Most of these studies have focussed on NbSe<sub>3</sub>, which undergoes two independent Peierls transitions to CDW states at  $T_{P_1} \approx 145$  K and at  $T_{P_2} \approx 59$  K. The most widely studied dopant has been Ta, which is isoelectronic with Nb.

Experimentally [4,5], the structure of the  $\mathbf{Q}_1$  CDW in Ta-doped NbSe<sub>3</sub> is quite well described by a Ginzburg-Landau field theory [11]. The effective Hamiltonian which describes the phase behavior of the  $\mathbf{Q}_1$  CDW at low temperatures can be written as [7]

$$\mathcal{H}_\phi = \int d^d \mathbf{x} \left\{ \psi^2 (\boldsymbol{\xi} \cdot \nabla \phi(\mathbf{x}))^2 + \psi h(\mathbf{x}) \phi(\mathbf{x}) \right\}, \quad (1)$$

where  $\psi$  is the amplitude of CDW order parameter,  $\phi(\mathbf{x})$  is the phase of the CDW order parameter,  $\boldsymbol{\xi}$  is the amplitude coherence length, and  $h(\mathbf{x})$  is the quenched random field.

Using  $\mathcal{H}_\phi$  and the assumption that  $h(\mathbf{x})$  obeys Gaussian statistics, the phase-phase correlation function in three dimensions is [7,8]  $\langle e^{i[\phi(\mathbf{x}_1) - \phi(\mathbf{x}_2)]} \rangle \sim e^{-g(\mathbf{x}_1 - \mathbf{x}_2)}$ , where

$$g(\mathbf{x}) = \int_{k=1/L}^{k=1/\xi} \frac{d^3 k}{(2\pi)^3} \frac{n_i h_0^2}{4\xi^4 \psi^2 k^4} \{1 - \cos(\mathbf{k} \cdot \mathbf{x})\}, \quad (2)$$

and  $L$  is the system size. At large separations,  $\langle e^{i[\phi(\mathbf{x}_1) - \phi(\mathbf{x}_2)]} \rangle \sim e^{-|\mathbf{x}_1 - \mathbf{x}_2|/\ell}$ , where the correlation length is given by  $\ell = \frac{32\pi\xi^4\psi^2}{n_i h_0^2}$ .

In order to provide a framework for discussing the experimental results, we first consider the consequences of random fields on the measured profiles. In an x-ray scattering experiment on a CDW system at low temperatures, the static structure factor  $\mathcal{S}(\mathbf{q})$  is proportional to the spatial Fourier transform of the phase-phase correlation function [5]. Thus, at low temperatures  $\mathcal{S}(\mathbf{q})$  exhibits Lorentzian squared fluctuations centered about the CDW satellite reflection positions.

The experimentally measured profile is the convolution of  $\mathcal{S}(\mathbf{q})$  with the resolution function of the diffractometer,  $\mathcal{R}(\boldsymbol{\zeta})$ . If the sample has nontrivial mosaic structure, that must also be convolved into the resolution function. The form of  $\mathcal{R}(\boldsymbol{\zeta})$  can be calculated from first principles [12]. To obtain a simple analytic form of the resolution function, we assume (i) that the line shape of the rocking curves of the monochromator and analyzer are Gaussians, (ii) that the half-widths of these curves are determined by the Darwin width of Si(111),

(*iii*) that the angular profile of the wiggler beam is Gaussian, and (*iv*) that the angular divergence of the wiggler beam is that same as that of a bend magnet at the critical wavelength. The assumed Gaussian line shapes allow the integrals to be done analytically. The result is then transformed from angle space to reciprocal space, and fit to an anisotropic Gaussian line shape. The half widths are  $W_{\parallel} = 2.08 \times 10^{-4} \text{\AA}^{-1}$  and  $W_{\perp} = 2.06 \times 10^{-5} \text{\AA}^{-1}$ . The long axis is rotated by  $7.48^{\circ}$  from the longitudinal direction. The ellipse describing the half height of  $R(\zeta)$  is plotted in the inset to Fig. 1. We will show below that the intrinsic scattering is, in fact, much narrower than the resolution of the diffractometer in both the  $q_{\parallel}$  (longitudinal) and the  $q_z$  (out of scattering plane) directions. Therefore, the directions orthogonal to a transverse scan are integrated away and the dimensionality of the Fourier transform is effectively lowered from three to one [5]. Thus, the observed line shape is given by the one-dimensional convolution of the intrinsic scattering with the resolution function. Since the one-dimensional Fourier transform of an exponentially decaying correlation function is a simple Lorentzian, the observed scattering will be the convolution of a Gaussian resolution function and a Lorentzian structure factor.

The experiments were carried out using a six-circle diffractometer on the X-25 wiggler beam line at the National Synchrotron Light Source. The beam line optics include a toroidally focusing mirror, a double crystal Si(111) monochromator, and a triple-bounce channel-cut Si(111) analyzer crystal. Non-dispersive rocking curves of the analyzer produced Darwin-limited behavior. Our samples were single-crystal whiskers of NbSe<sub>3</sub> lightly doped with Ta ( $\frac{R(300\text{ K})}{R(4\text{ K})} \equiv r_R \approx 45$ ). The macroscopic sample dimensions were approximately  $2 \mu\text{m} \times 20 \mu\text{m} \times 5 \text{ mm}$ . The crystal structure of NbSe<sub>3</sub> is monoclinic and the real space lattice constants [13] are  $a = 10.009 \text{\AA}$ ,  $b = 3.4805 \text{\AA}$ ,  $c = 15.629 \text{\AA}$ , and  $\beta = 109.47^{\circ}$ . We studied only the  $T_{P_1}$  CDW whose wave vector is  $\mathbf{Q}_1 = [0 \ Q_1 \ 0]$ , where  $Q_1 \approx 0.243$  and varies slightly with temperature [14]. The samples were mounted using silver paint across a 3.5 mm hole in an alumina substrate and studied in transmission. Sample cooling was provided by a closed-cycle helium refrigerator. All of the data presented in this paper were collected at 70 K.

Figure 1 shows a scan in the  $\mathbf{b}^*$  direction through the  $[0 \overline{1+Q_1} 0]$  CDW satellite of sample #1. During a typical injection cycle, the stored electron beam current decayed from roughly 200 to 150 mA. The data was collected for a constant number of incident x-rays and is plotted as counts per sec assuming 100 mA in the storage ring. The half-width at half-maximum (HWHM) of the scan in the  $\mathbf{b}^*$  direction is  $1.2 \times 10^{-4} \text{\AA}^{-1}$ , which is 10% smaller than the value obtained from the cut through the *a priori* resolution function appropriate for a resolution-limited peak. This cut is indicated by the arrows in the inset to Fig. 1. Thus, as claimed above, this scan is *completely* resolution limited. Figures 2 and 3 show scans through the  $[0 \overline{1+Q_1} 0]$  CDW satellite in the  $\mathbf{a}^*$  direction for two different samples. The Gaussian resolution function in the  $\mathbf{a}^*$  direction, which now includes the sample mosaic as measured at the  $[0 \overline{2} 0]$  Bragg peak, is indicated by the dot-dashed line in the inset of each figure and the values of the HWHM,  $W_R$ , are listed in table I. The dashed lines in Figs. 2 and 3 are the best fit to the convolution of a simple Lorentzian and the Gaussian resolution for the two samples. The background level  $I_{BG}$  has been constrained to remain at or above the measured value of the background. A small asymmetry factor has been included. This factor improves the quality of the fit but does not affect the values of the other parameters. A casual inspection of Figs. 2 and 3 reveals two important points. First, the high brightness wiggler source associated with X-25 allowed us to obtain data over four decades of intensity, roughly two decades better than in previous measurements [5]. Second, this extra dynamic range clearly reveals that the simple Lorentzian line shape overestimates the scattering in the wings.

It is not surprising that the tails do not agree with a simple Lorentzian line shape. The exponential decay of the phase-phase correlation function is valid only at large separations, breaking down at small separations. The magnitude of this discrepancy can be made quantitative by considering the Taylor series expansion of Eq. (2) about  $x = 0$ .

$$g(x) \approx \frac{2}{3\pi\ell} \left( \frac{1}{\xi} - \frac{1}{L} \right) x^2 + \mathcal{O}(x^4) \quad (3)$$

In contrast to the asymptotic form, the full functional form of  $g(x)$  approaches the origin

with zero slope.

Previously, high resolution x-ray scattering studies of the structure of the Pt(001) surface [17] and high stage Br-intercalated graphite [18] have observed that it is necessary to approximate  $g(\mathbf{x})$  in a manner which preserves the *functional* form at both large and small distances [19]. In our particular case, this can be done by letting  $g(x) = \sqrt{a^2 + x^2}/\ell$ . As before, the observed line shape is given by a one-dimensional convolution in reciprocal space of the static structure factor with the resolution function. The one-dimensional static structure factor describing transverse scans through the CDW satellite produced by this model is [15]

$$\mathcal{S}(q_{\perp}) \sim \int_{-\infty}^{\infty} dx e^{iq_{\perp}x} \exp\left[-\frac{\sqrt{a^2 + x^2}}{\ell}\right] \quad (4)$$

$$= \frac{2a/\ell}{\sqrt{\ell^{-2} + q_{\perp}^2}} K_1\left(a\sqrt{\ell^{-2} + q_{\perp}^2}\right) \quad (5)$$

where  $K_1(x)$  is the modified Bessel function of order 1. For small arguments,  $K_1(x) \approx x^{-1}$  and the simple Lorentzian form is recovered. For large arguments,  $K_1(x) \approx \frac{\pi}{\sqrt{2\pi x}} \exp(-x)$  and the scattering decays exponentially. Qualitatively, introducing a cutoff at small  $x$  reduces the scattering in the wings.

The solid lines in Figs. 2 and 3 are the best fit to the convolution of Eq. (5) with the Gaussian resolution functions shown in the insets. The agreement between the fits and the data is striking. Quantitatively, for sample #1, the goodness-of-fit parameter  $\chi^2$  changes from 26.7 to 5.5 when the parameter  $a$  is allowed to rise up from zero. The best fit values for  $a$  and  $\ell$  for the two samples studied are listed in Table I. These best fit values of  $\ell$  are consistent with those obtained by DiCarlo, *et al.* in Ref. 5.

As a test of our assertion that the intrinsic line shape is nominally a Lorentzian because we have integrated over the  $q_{\parallel}$  direction, we fit these data to the convolution of the resolution function with a Lorentzian raised to an arbitrary power  $\eta$ . Similar to a cut off at small  $x$ , increasing the value of  $\eta$  suppresses the scattering in the wings. However, the data is best described by a Lorentzian. Quantitatively, for sample #1, the best fit value of the exponent

was  $\eta \approx 1.09 \pm 0.04$  with  $\chi^2 \approx 13$ , roughly twice that obtained using Eq. (5), and excluding a Lorentzian to the  $\frac{3}{2}$  line shape.

The principal result of our line shape analysis, the existence of a second length scale, is not sensitive to our assumption of a Gaussian resolution function. This is quite important since the true resolution function is certainly not expected to be Gaussian. Both dynamical diffraction [12] and thermal diffuse scattering [16] theory predict that a Bragg peak should have tails which decay only as  $q^{-2}$ . Due to the convolution, the observed scattering associated with a resolution function with wings would be enhanced relative to the Gaussian prediction. But, since the predicted effect is a *decrease* in the scattering, our essential result is insensitive to such tails.

Our line shape analysis of the data demonstrates that high frequency phase fluctuations are suppressed in NbSe<sub>3</sub>. This suppression is consistent with the predictions of the Ginzburg-Landau field theory which specifically excludes phase fluctuations with spatial frequencies greater than  $1/\xi$ . The connection between our simple approximate form of  $g(x)$  and the exact formulation can be examined by equating the Taylor series expansion of  $\sqrt{a^2 + x^2}/\ell$  with Eq. (3), yielding  $a = (3\pi/4)\xi$ . Thus, combining our two data sets, we find that the amplitude coherence length in the  $\mathbf{a}^*$  direction is  $\xi_{\mathbf{a}^*} = 34.4 \pm 10.3\text{\AA}$ .

The observation that high frequency phase fluctuations are suppressed has implications for our physical picture of the pinning mechanism, supporting the following picture which is based on the notion of a Friedel oscillation [20]. The same divergence of the susceptibility which drives the Peierls transition causes the conduction electron density to respond to a point impurity by creating an oscillating charge density with wavenumber  $2k_F$ . Of course these oscillations cannot continue to infinite distance in a real sample. In general, we expect an exponential decay of the form  $e^{-r/\xi}$  for these oscillations due to scattering of the conduction electrons by other defects. The minimum value of the mean free path is, by definition, the amplitude coherence length  $\xi$ . Thus, a pinning site prefers not only a particular value of the phase, but that the phase be constant over a region of characteristic size  $\xi$ . In contrast to the physical description usually given for strong pinning in which the phase gradients are

largely confined to a small region surrounding an individual impurity [21], phase gradients are expelled from the neighborhood of impurity sites.

Both strong and weak pinning theories are subsumed within the random field description; however, the structure of the CDW is determined primarily by the statistics of the random field, not its intensity. In our ongoing work studying the kinetics of CDW systems, the more general random field description is expected to be the most useful.

The authors thank R.E. Thorne for providing the NbSe<sub>3</sub> samples. This work was supported by Cornell's Materials Science Center (NSF Grant No. DMR-88-1858-A02) and by the NSF (Grant No. DMR-92-57466). Additional support was provided by the AT&T Foundation. These data were collected on beam line X25 at the National Synchrotron Light Source, Brookhaven National Laboratory, which is supported by the U.S. Department of Energy, Division of Materials Sciences and Division of Chemical Sciences (Contract No. DE-AC02-76CH00016).



## REFERENCES

- [1] A.B. Harris, J. Phys. C **7**, 1671 (1974); G. Grinstein and A. Luther, Phys. Rev. B **13**, 1329 (1976).
- [2] Y. Imry and S.-K. Ma, Phys. Rev. Lett. **35**, 1399 (1975).
- [3] L.D. Landau & E.M. Lifshitz, *Statistical Physics*, (Pergamon Press, New York) 1980.
- [4] E. Sweetland, C.-Y. Tsai, B.A. Wintner, J.D. Brock, and R.E. Thorne, Phys. Rev. Lett. **63**, 2841 (1989).
- [5] D. DiCarlo, R.E. Thorne, E. Sweetland, M. Sutton, and J.D. Brock, Phys. Rev. B (in press).
- [6] P. Debye, H.R. Anderson, Jr., and H. Brumberger, J. App. Phys. **28**, 679 (1957).
- [7] L.J. Sham and Bruce R. Patton, Phys. Rev. B **13**, 3151 (1976).
- [8] K.B. Efetov and A.I. Larkin, Sov. Phys. JETP **45**, 1236 (1978).
- [9] For comprehensive reviews of the electronic properties of CDW systems see P. Monceau, in **Electronic Properties of Quasi-One-Dimensional Materials** (Reidel, Dordrecht, 1985), Pt. II, p. 139; G. Grüner, Rev. Mod. Phys. **60**, 1129 (1988).
- [10] R.E. Thorne, Phys. Rev. B **45**, 5804 (1992). See also, F. Levy and H. Berger, J. Cryst. Growth **61**, 61 (1983).
- [11] H. Fukuyama and P.A. Lee, Phys. Rev. B **17**, 535 (1978); P.A. Lee and T.M. Rice, Phys. Rev. B **19**, 3970 (1979).
- [12] R.W. James, *The Optical Principles of The Diffraction of X-rays*, (Ox Bow Press, Woodbridge, 1962).
- [13] J.L. Hodeau, M. Marezio, C. Roucau, R. Ayroles, A. Meerschaut, J. Rouxel, and P. Monceau, J. Phys. C **11**, 4117 (1978).

- [14] A.H. Moudden, J.D. Axe, P. Monceau, and F. Levy, Phys. Rev. Lett. **65**, 223 (1990).
- [15] This integral is Eq. 8.338(2) in I.S. Gradshteyn and I.M. Ryzhik, *Table of Integrals, Series, and Products*, (Academic Press, New York, 1980), p. 938.
- [16] B.E. Warren, *X-ray Diffraction*, (Dover, New York, 1990).
- [17] D.L. Abernathy, S.G.J. Mochrie, D.M. Zehner, G. Grubel, and Doon Gibbs, Phys. Rev. Lett. **69**, 941 (1992).
- [18] S.G.J. Mochrie, A.R. Kortan, R.J. Birgeneau, and P.M. Horn, Z. Phys. B **62**, 79 (1985).
- [19] References 17 and 18 stressed that it was important to keep  $g(0) = 0$ ; however, the present work clearly demonstrates that it is the functional form, not the absolute value, which must be maintained. An incorrect absolute value can simply be rescaled away by a constant multiplicative factor. An incorrect functional form always produces an incorrect line shape.
- [20] Walter A. Harrison, *Solid State Theory*, (Dover, New York, 1980).
- [21] J.R. Tucker, W.G. Lyons, and G. Gammie, Phys. Rev. B **38**, 1148 (1988); J.R. Tucker, Phys. Rev. B **40**, 5447 (1989).

## FIGURES

FIG. 1. Scan in the  $\mathbf{b}^*$  direction through the  $[0 \overline{1+Q_1} 0]$  CDW satellite of sample #1. Error bars represent counting statistics. Solid line is the best fit to a Gaussian. Inset shows ellipse depicting the half-height of the *a priori* resolution function. The arrows indicate the value predicted for the width.

FIG. 2. Scan in the  $\mathbf{a}^*$  direction through the  $[0 \overline{1+Q_1} 0]$  CDW satellite of sample #1. The dashed line is the best fit to the convolution of a Lorentzian with the Gaussian resolution. The solid line is the best fit to the convolution of Eq. (10) with the Gaussian resolution. The inset shows the central portion of the scan on a linear scale.

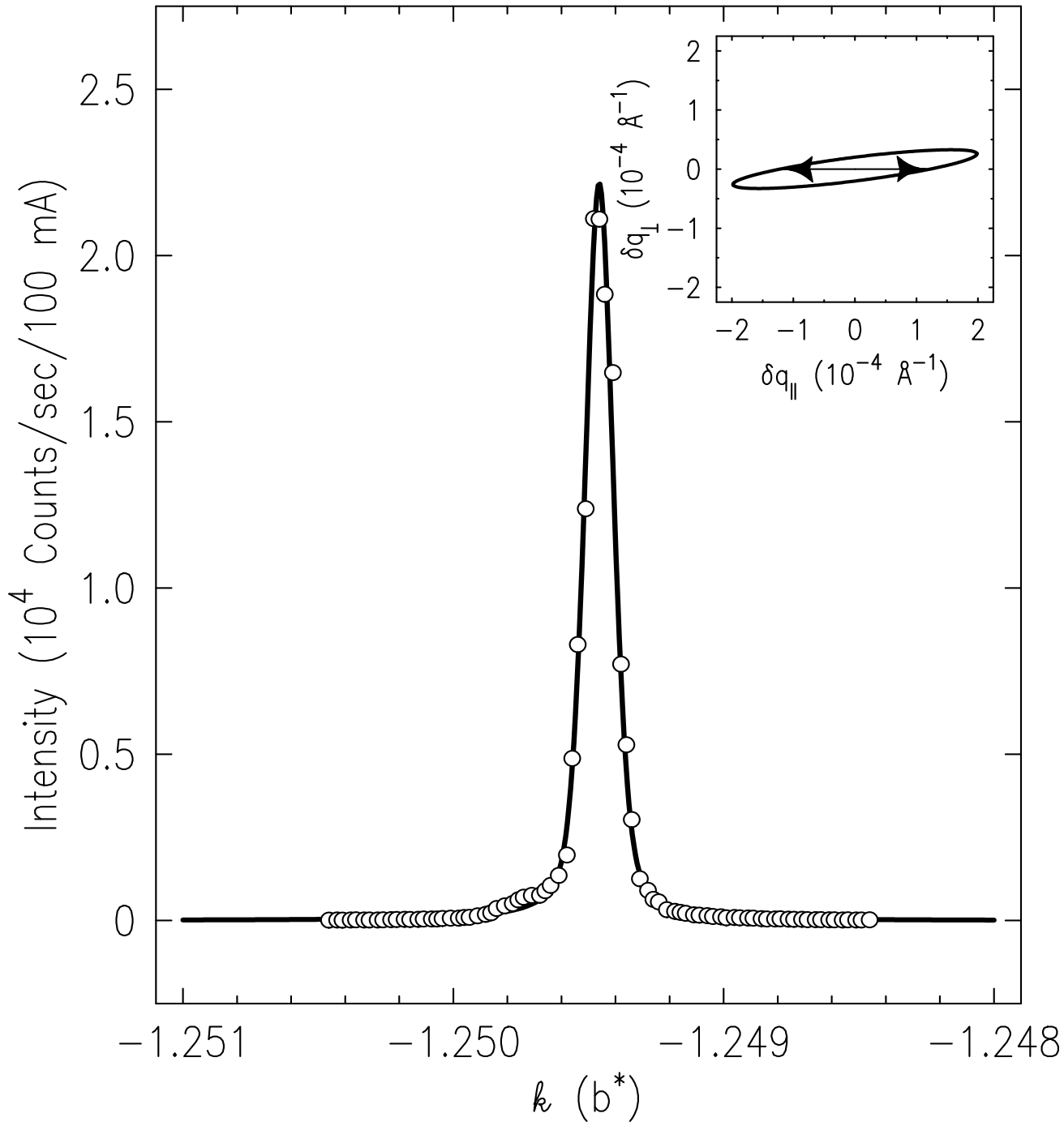
FIG. 3. Scan in the  $\mathbf{a}^*$  direction through the  $[0 \overline{1+Q_1} 0]$  CDW satellite of sample #2.

TABLES

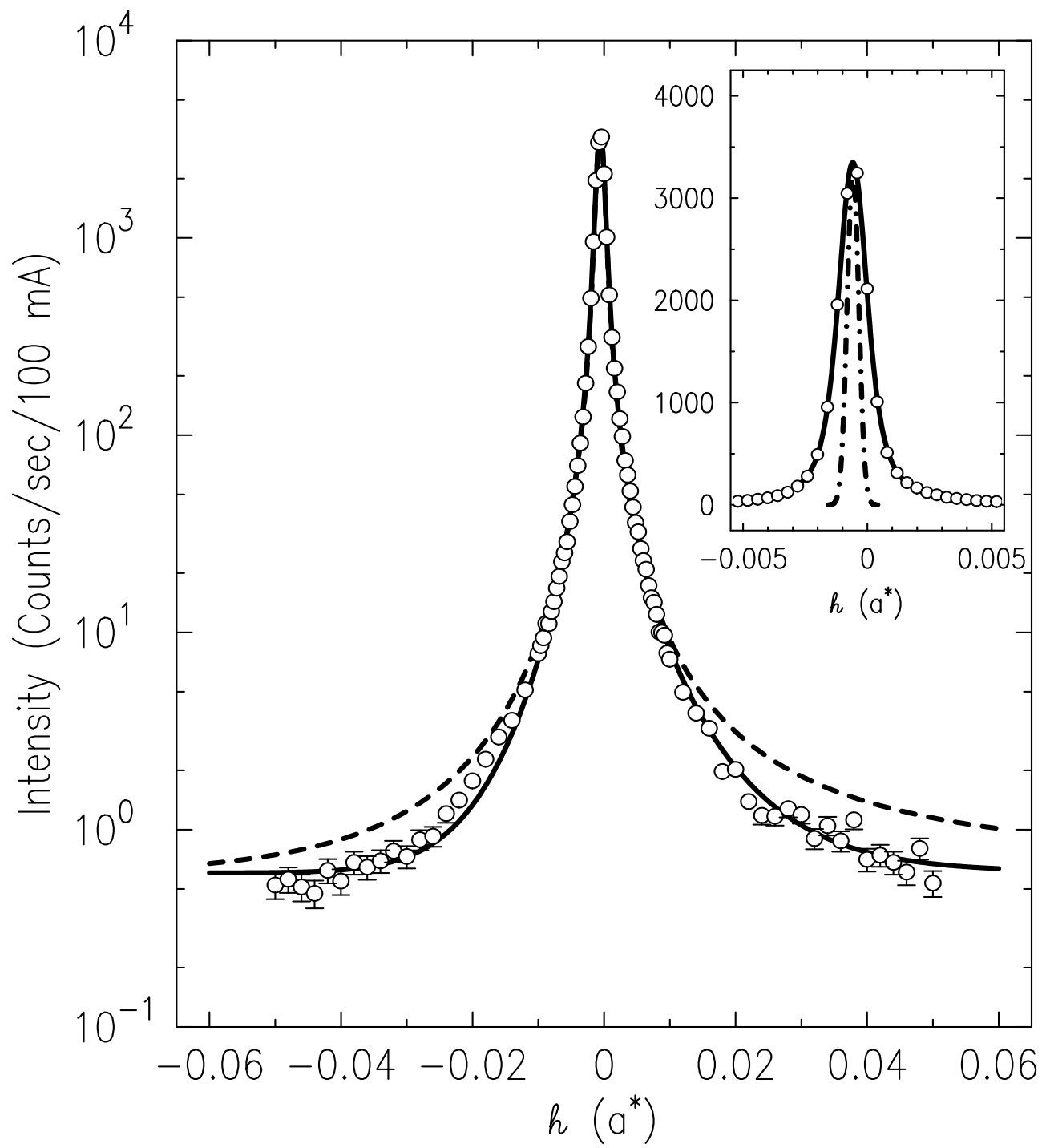
TABLE I. Summary of parameters describing NbSe<sub>3</sub> samples lightly doped with Ta ( $r_R \approx 45$ ).

The errors on the parameters represent  $1\text{-}\sigma$  confidence limits of the nonlinear least squares fit.

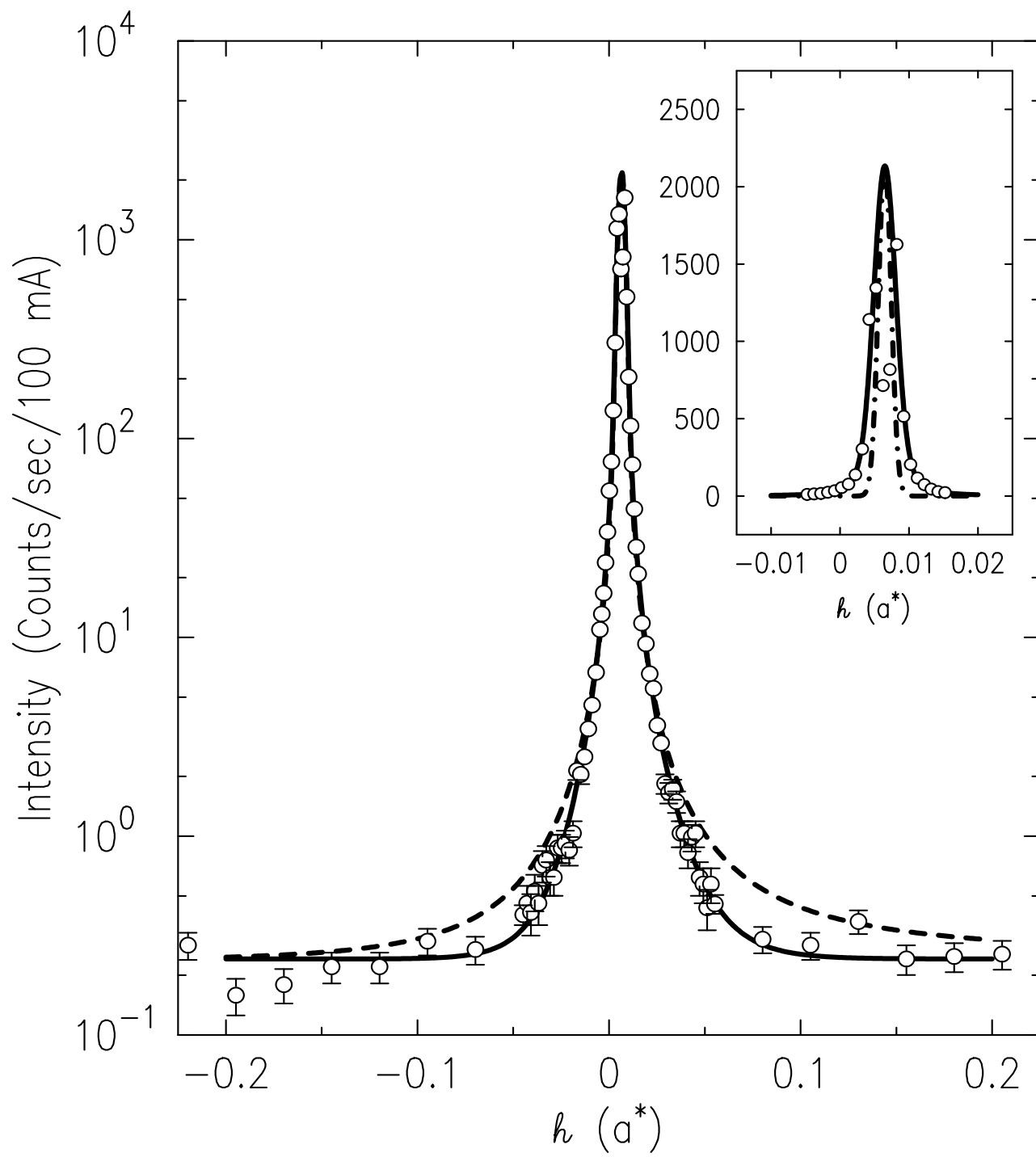
	Sample #1	Sample #2
$a$	$102 \pm 30 \text{ \AA}$	$60 \pm 38 \text{ \AA}$
$l_{\mathbf{a}^*}$	$3\,275 \pm 175 \text{ \AA}$	$3\,050 \pm 400 \text{ \AA}$
$W_R$ (HWHM)	$3.3 \times 10^{-4} \text{ \AA}^{-1}$	$1.32 \times 10^{-3} \text{ \AA}^{-1}$
$I_{BG}$	0.61 counts/sec	0.24 counts/sec



Brock, et al.: Figure 1



*Brock, et al.: Figure 2*



*Brock, et al.: Figure 3*